

# Raspberry-like poly( $\gamma$ -glutamic acid) hydrogel particles for pH-dependent cell membrane passage and controlled cytosolic delivery of antitumor drugs

Sun-Hee Cho<sup>1,\*</sup>  
 Ji Hyeon Hong<sup>2,\*</sup>  
 Young-Woock Noh<sup>1</sup>  
 Eunji Lee<sup>2</sup>  
 Chang-Soo Lee<sup>3</sup>  
 Yong Taik Lim<sup>1</sup>

<sup>1</sup>SKKU Advanced Institute of Nanotechnology, School of Chemical Engineering, Sungkyunkwan University, Suwon, Gyeonggi-do, <sup>2</sup>Graduate School of Analytical Science and Technology, Chungnam National University, <sup>3</sup>Hazards Monitoring Bionano Research Center, Korea Research Institute of Bioscience and Biotechnology, Yuseong-gu, Daejeon, Republic of Korea

\*These authors contributed equally to this work

Correspondence: Yong Taik Lim  
 SKKU Advanced Institute of Nanotechnology, School of Chemical Engineering, Sungkyunkwan University, 2066 Seobu-ro, Suwon, Gyeonggi-do 16419, Republic of Korea  
 Tel +82 31 299 4172  
 Fax +82 31 299 4119  
 Email yongtaik@skku.edu

Chang-Soo Lee  
 Hazards Monitoring Bionano Research Center, Korea Research Institute of Bioscience and Biotechnology, 125 Gwahak-ro Yuseong-gu, Daejeon 34141, Republic of Korea  
 Tel +82 42 879 8446  
 Fax +82 42 879 8594  
 Email cslee@kribb.re.kr

**Abstract:** In this research, we synthesized bioderived poly(amino acid) hydrogel particles that showed pH-dependent membrane-disrupting properties and controlled cytosolic delivery of antitumor drugs. Poly( $\gamma$ -glutamic acid) ( $\gamma$ -PGA) that has been produced extensively using bacteria, especially those of *Bacillus subtilis* species, was modified with cholesterol ( $\gamma$ -PGA/Chol), and the  $\gamma$ -PGA/Chol conjugates were used to form polymeric nanoparticles the size of  $21.0 \pm 1.1$  nm in aqueous solution. When the polymeric nanoparticles were mixed with doxorubicin (Dox), raspberry-like hydrogel particles (RBHPs) were formed by the electrostatic interaction between the cationically charged Dox and the anionically charged nanoparticles. The average size and surface charge of the RBHPs in aqueous solution were  $444.9 \pm 122.5$  nm and  $-56.44$  mV, respectively. The loaded amount of Dox was approximately  $63.9 \mu\text{g}/\text{mg}$  of RBHPs. The RBHPs showed controlled drug release behavior in both in vitro and ex vivo cell-based experiments. Through fluorescence microscopy and fluorescence-activated cell sorting, the cellular uptake of RBHPs into human cervical cancer cells (HeLa) was analyzed. The cytotoxic effect, evaluated by the methyl tetrazolium salt assay, was dependent on both the concentration of RBHPs and the treatment time. The pH-dependent membrane-disrupting properties of the RBHPs and the subsequent cytosolic delivery of Dox were evaluated using a standard hemolysis assay. Upon an increase in hydrophobicity at the lysosomal acidic pH, RBHPs could easily interact, penetrate cell membranes, and destabilize them. Taken together, the data suggested that RBHPs could be used as drug delivery carriers after loading with other therapeutic drugs, such as proteins or small interfering RNA for cancer therapy.

**Keywords:** hydrogel particles, controlled release, endosomal escape, antitumor

## Introduction

The design and synthesis of nanoparticles that can detect and treat specific diseases have been concerns in both biotechnology and medicine fields. For the effective encapsulation and delivery of therapeutic drugs, various types of nanomaterials (such as polymeric micelles, liposomes, emulsions, and hydrogel nanoparticles) have been developed.<sup>1-9</sup> Nanoparticles facilitate the encapsulation of water-insoluble drugs and their controlled release into disease-specific target cells. In particular, self-assembled polymeric nanoparticles have been explored as smart drug delivery systems that can deliver anticancer drugs into specific tumor cells.<sup>9,10</sup> Amphiphilic polymer chains can form self-assembled nanoparticles with a hydrophilic outer shell and a hydrophobic inner core in aqueous solution by the hydrophilic-hydrophobic balance. During the

self-assembling process, hydrophobic anticancer drugs can be encapsulated into the hydrophobic core.<sup>11,12</sup> Hydrogel polymer nanoparticles contain three-dimensional networks of chemically or physically cross-linked polymer chains.<sup>11,13</sup> Due to the water-absorbing and swelling properties of hydrogel particles, various kinds of hydrophilic drugs and biomolecules can be easily loaded into the hydrogel nanoparticles, in addition to the hydrophobic anticancer drugs. The loading and release of encapsulated drugs in hydrogel polymer nanoparticles can be controlled by various biological stimuli, pH, temperature, and light.<sup>6,14–19</sup>

For high therapeutic efficacy and minimal side effects, the anticancer drug delivery carrier should tightly retain the drug, efficiently reach the tumor, and then quickly enter the tumor cells and release the drug. After reaching tumor cells, drug delivery carriers are generally internalized by endocytosis and routed to endosomes and thereafter to acidic lysosomes. The encapsulated drug must quickly diffuse into the cytosol because the harsh environment of lysosomes can degrade drugs sensitive to acid or lysosomal enzymes. Nanoparticles or chemical linkers sensitive to the lysosomal acidic pH have been used to trigger drug release. Amine-containing hydrophobic polymers such as polyhistidine can also be protonated in acidic lysosomes, thereby releasing the drug. The polymers may additionally have endosomal membrane-disruptive activity induced by a “proton sponge” mechanism, resulting in disruption of the lysosomal membrane and release of drug into the cytosol. Poly(propylacrylic acid) has also been shown to disrupt endosomes at  $\leq$ pH 6.5, causing the cytosolic release of cargo molecules.<sup>1–4</sup>

In this study, we have developed a novel type of hydrogel particle, for the cytosolic delivery of antitumor drugs, by the electrostatic self-assembly of bioderived poly( $\gamma$ -glutamic acid) ( $\gamma$ -PGA)-based polymeric nanoparticles with antitumor drugs.  $\gamma$ -PGA is a highly anionic polypeptide that is synthesized naturally by microbial species, most prominently by various bacilli, and has shown excellent biocompatibility and noncytotoxicity.  $\gamma$ -PGA can either be composed of repeating units of L-glutamic acid, D-glutamic acid, or both.<sup>20,21</sup>  $\gamma$ -PGA polymer has attracted much interest as a promising biomaterial for a variety of applications, such as applications in medicine, cosmetics, and the food industry.<sup>22–26</sup> Cholesterol, which is an essential structural component of mammalian cell membranes, is a hydrophobic moiety that has also been used to form self-assembling nanoparticles.<sup>20,24</sup> Because  $\gamma$ -PGA has a lot of carboxyl groups, hydrophobic moieties such as cholesterol can be conjugated ( $\gamma$ -PGA/Chol)

and amphiphilic  $\gamma$ -PGA can be synthesized. In addition, the abundant carboxyl groups of  $\gamma$ -PGA can be deprotonated or protonated depending on the pH of the solution. Thus, due to the amphiphilic and pH-dependent properties of  $\gamma$ -PGA/Chol conjugates, they can be used as drug carriers that facilitate drug delivery within a specific pH range. Herein, biosynthetic  $\gamma$ -PGA was modified with cholesterol, which formed self-assembled polymer nanoparticles and showed negative character at neutral pH due to the deprotonated carboxylate groups. In this study, we fabricated submicron-sized raspberry-like hydrogel particles (RBHPs) by combining an antitumor drug and 20 nm-sized  $\gamma$ -PGA/Chol nanoparticles. The hydrogel particles were formed by the electrostatic interaction between the cationically charged anticancer drug and the anionically charged nanoparticles (Figure 1). In the synthesis process, the nanoparticles acted as building blocks, and the antitumor drug molecules made bridges between the building blocks, serving as cross-linkers. Finally, we also investigated the intracellular delivery of RBHP(Dox) and release of the encapsulated anticancer drugs into the cytosol of cancer cells.

## Materials and methods

### Materials

The  $\gamma$ -PGA (acid form, 50 kDa) was obtained from Bioleaders Corporation (Daejeon, Republic of Korea). Cholesteryl chloroformate, 1,1'-carbonylbis-1H-imidazole (CDI), and ethylenediamine (EDA) were purchased from Sigma-Aldrich Co (St Louis, MO, USA). Doxorubicin hydrochloride (Dox) was obtained from Boryung Pharmaceutical Co (Ansan, Republic of Korea).

### Methods

#### Synthesis of cholesterol-NH<sub>2</sub>

Cholesterol amine was synthesized by conjugation of cholesterol to EDA, as previously described.<sup>22</sup> Briefly, cholesteryl chloroformate (2.25 g, 5 mmol) in anhydrous toluene (50 mL) was slowly added to EDA (16.7 mL, 250 mmol) in anhydrous toluene (250 mL) at 0°C, and the solution was allowed to react at room temperature for 16 h. After the reaction, the mixture was washed with deionized water, dried over anhydrous magnesium sulfate, and evaporated by rotary evaporation. The white powder was co-dissolved in dichloromethane (50 mL) with methanol (50 mL). The solution was filtered to remove the biscarbamate by syringe filtration (1  $\mu$ m, polytetrafluoroethylene). The filtrate was then evaporated by rotary evaporation to obtain the product, and proton nuclear

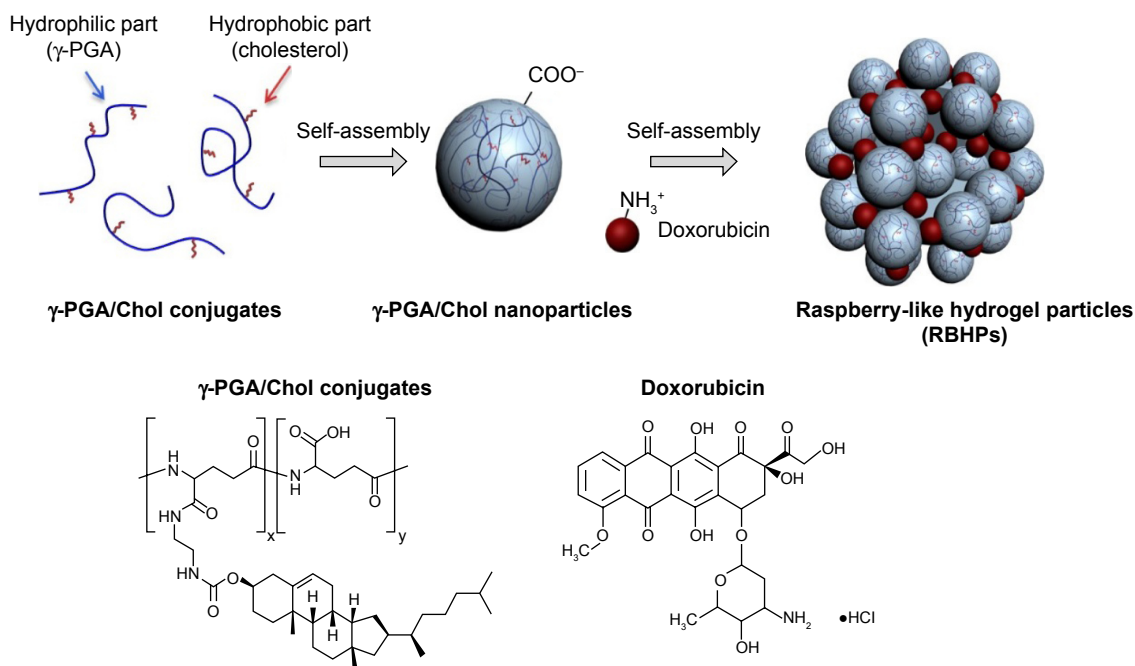


**Figure 1** Scheme for the synthesis of RBHPs.

**Notes:**  $\gamma$ -PGA was modified with cholesterol ( $\gamma$ -PGA/Chol), and the  $\gamma$ -PGA/Chol conjugate was used to form polymeric nanoparticles in aqueous solution. When the polymeric nanoparticles were mixed with Dox, RBHPs were formed by the electrostatic interaction between the cationically charged Dox and the anionically charged nanoparticles.

**Abbreviations:** RBHPs, raspberry-like hydrogel particles;  $\gamma$ -PGA, poly( $\gamma$ -glutamic acid); Chol, cholesterol; Dox, doxorubicin.

magnetic resonance ( $^1\text{H}$ -NMR) spectroscopy was used to characterize the product:  $^1\text{H}$ -NMR (deuterated chloroform [ $\text{CDCl}_3$ ])  $\delta$  0.7, 1.0 (s, each 3H, Me), 0.9 (d, 6H, Me), 0.9 (d, 3H, Me), 1.0–1.7 (m, 23H, CH and NH), 1.8–2.1 (m, 5H), 2.2–2.4 (m, 2H), 2.8 (t, 2H,  $\text{NH}_2\text{CH}_2$ ), 3.1 (q, 2H,  $\text{NHCH}_2$ ), 4.4–4.6 (m, 1H, OCH), 4.9–5.0 (m, 1H,  $\text{NHCOO}$ ), and 5.3 (d, 1H,  $\text{CHdC}$ ).

### Synthesis of $\gamma$ -PGA/Chol conjugate

The  $\gamma$ -PGA/Chol conjugate was synthesized as follows. Briefly, both cholesterol- $\text{NH}_2$  (46 mg, 0.097 mmol) dissolved in 10 mL of tetrahydrofuran (THF) and CDI (63 mg, 0.3876 mmol) were slowly added to  $\gamma$ -PGA (500 mg, 3.876 mmol) dissolved in 10 mL of dimethyl sulfoxide (DMSO) with stirring at  $40^\circ\text{C}$  for 18 h. After the reaction, the solution was cooled to room temperature and evaporated by rotary evaporation to remove the THF. And then, 100 mL of acetone was poured into the residue. After centrifugation, the precipitate was collected and dried at  $40^\circ\text{C}$ . The product was dissolved in deionized water, followed by the addition of  $\text{NaHCO}_3$  and stirring for 3 h at  $40^\circ\text{C}$ . Amberlite IR-120H beads were used for ion exchange treatment of the solution. After filtration with the Amberlite beads, the solution was dialyzed

using a cellulose membrane tube (molecular weight cutoff [MWCO]: 12–14 kDa) in deionized water for 2 days. The solution was freeze-dried, and  $^1\text{H}$ -NMR spectroscopy was used to characterize the product:  $^1\text{H}$ -NMR (DMSO- $d_6$ )  $\delta$  0.8–1.5 (br,  $\text{CH}_3$ ,  $\text{CH}_2$ , and CH of cholesterol), 1.7, 1.9 (br,  $\beta$ - $\text{CH}_2$  of  $\gamma$ -PGA), 2.2 (br,  $\gamma$ - $\text{CH}_2$  of  $\gamma$ -PGA), 3.0–3.1 (br,  $\text{NHCH}_2$ ), 4.1–4.3 (br,  $\alpha$ -CH of  $\gamma$ -PGA), and 5.3 (d,  $\text{CH}=\text{C}$ ).

### Preparation and characterization of hydrogel particles

The hydrogel particles composed of  $\gamma$ -PGA/Chol nanoparticles and Dox were prepared via the following steps: 1) 10 mL of Dox solution (1 mg/mL in deionized water) was added to  $\gamma$ -PGA/Chol nanoparticles (100 mg) dissolved in 10 mL of deionized water. 2) The solution was stirred for 3 h, filtered using a  $0.8\ \mu\text{m}$  syringe filter, and freeze-dried. To quantify the concentration of encapsulated Dox in the hydrogel particles, 0.4 mL of 10% sodium dodecyl sulfate and 3 mL of DMSO were added to 0.6 mL of hydrogel particles (1 mg/mL in deionized water). The amount of Dox was quantitatively determined using an ultraviolet–visible (UV-vis) spectrophotometer at 498 nm. The size distribution and surface charge of the  $\gamma$ -PGA/Chol nanoparticles and the

hydrogel particles containing both Dox and nanoparticles were measured by using dynamic light scattering (ELS-Z; Otsuka Electronics, Osaka, Japan). The morphology of the  $\gamma$ -PGA/Chol nanoparticles and the hydrogel particles containing both Dox and nanoparticles was observed by cryo-transmission electron microscopy.

### In vitro release test of hydrogel particles

To study the release of Dox from the hydrogel particles, 1 mL of hydrogel particles (1 mg/mL) was loaded into dialysis membrane tubes (MWCO: 12–14 kDa). The tubes were immersed in phosphate-buffered saline (PBS; pH 7.4) containing 0.5% (w/v) Tween 80 at 37°C. The dissolution medium (30 mL) was gently shaken at 50 rpm in a dark place. At specific times (1, 2, 3, 4, 6, 9, 12, 24, 48, and 72 h), the medium was replaced with fresh medium. The released amounts of Dox were determined using a UV-vis spectrophotometer at 498 nm.

### Cytotoxicity assay

HeLa cell (ATCC, Manassas, VA, USA) viability in the presence and absence of hydrogel particles was measured by the methyl tetrazolium salt (MTS) assay. HeLa cells were seeded at a density of  $5 \times 10^3$  per well (100  $\mu$ L) in flat-bottomed 96-well plates (Corning Costar, Cambridge, MA, USA). The cells were next treated with 0.05, 0.1, 0.5, or 1  $\mu$ g/mL hydrogel particles for 4 or 24 h. Untreated cells were used as controls. For the MTS assay, the CellTiter 96 Aqueous One Solution kit (Promega, Madison, WI, USA) was used, following the manufacturer's protocols. Briefly, the MTS reagent was added (10  $\mu$ L per well), and the plates were incubated for 4 h at 37°C. The absorbance was detected at 490 nm with a microplate reader (VersaMax™; Molecular Devices, Sunnyvale, CA, USA). All of the experiments were repeated three times independently.

### Evaluation of cellular uptake

To evaluate the intracellular delivery capacity of the hydrogel particles, HeLa cells were incubated with various concentrations of hydrogel particles (0.05, 0.1, 0.5, or 1  $\mu$ g/mL) in a  $\mu$ -slide 8-well microscopy chamber at a density of  $2 \times 10^4$  cells per well for 4 or 24 h at 37°C. The HeLa cells were then washed in cold PBS, fixed with 4% (w/v) paraformaldehyde solution for 20 min at room temperature and stained with 2  $\mu$ g/mL Hoechst 33342 (trihydrochloride trihydrate; Invitrogen Carlsbad, CA, USA) in PBS for 15 min. Fluorescence images were observed using a DeltaVision PD (Applied Precision Technologies, Issaquah, WA, USA) with

a filter set (excitation: 555/25, emission: 605/52) (Omega Optical, Brattleboro, VT, USA).

### Flow cytometry analysis

For the fluorescence-activated cell sorting analysis, HeLa cells were seeded in 6-well plates at a density of  $5 \times 10^5$  cells per well in culture medium. The culture medium was removed, and various concentrations (from 0.05 to 1  $\mu$ g/mL) of hydrogel particles were added to each well and incubated for 4 or 24 h. After incubation, all reagents were removed, and the cells were washed with PBS. After washing, the cells were trypsinized, and the supernatant was carefully removed. PBS was added to resuspend the cell pellet. The Dox fluorescence contained in the cells was analyzed using MACS® (Miltenyi Biotec, Bergisch Gladbach, Germany). A minimum of 10,000 events were collected. The data were analyzed using a MACS Quant Analyzer (Miltenyi Biotec).

### Hemolysis assay

The membrane-disruptive activity of the hydrogel particles was measured using a hemolysis assay. Sheep red blood cells (RBCs) were stored at 4°C in Alsever's solution. Prior to use, the RBCs were washed three times with saline and resuspended in saline at  $2 \times 10^8$  cells/mL. The hydrogel particles were dispersed at a concentration of 2 mg/mL in 50 mM MES (2-(N-morpholino)ethanesulfonic acid) buffer (pH 5.0–7.5) containing 0.15 M NaCl. An equal volume of the hydrogel particle solution was then added to the RBC suspension (final concentrations: hydrogel particles, 1 mg/mL; RBCs,  $1 \times 10^8$  cells/mL in 25 mM MES, 0.15 M NaCl). The samples were incubated in an aluminum block bath at 37°C for 1 h and then centrifuged at  $5,000 \times g$  for 5 min. To determine the hemolytic activity of the hydrogel particles, the absorbance of hemoglobin in the supernatant was measured with a microplate reader at 570 nm. To obtain 100% hemolysis, the RBCs ( $1 \times 10^8$  cells/mL) were lysed with 0.2% Triton X in water.

## Results and discussion

### Preparation and characterization of RBHPs

Figure 1 describes the synthesis of RBHPs by the electrostatic self-assembly of  $\gamma$ -PGA-based polymer nanoparticles with an anticancer drug. The submicron-sized RBHPs were formed by the electrostatic interaction between the cationically charged anticancer drug and the anionically charged  $\gamma$ -PGA/Chol nanoparticles. Figure 2 shows the chemical synthetic strategy for the self-assembled  $\gamma$ -PGA/Chol nanoparticles based on the

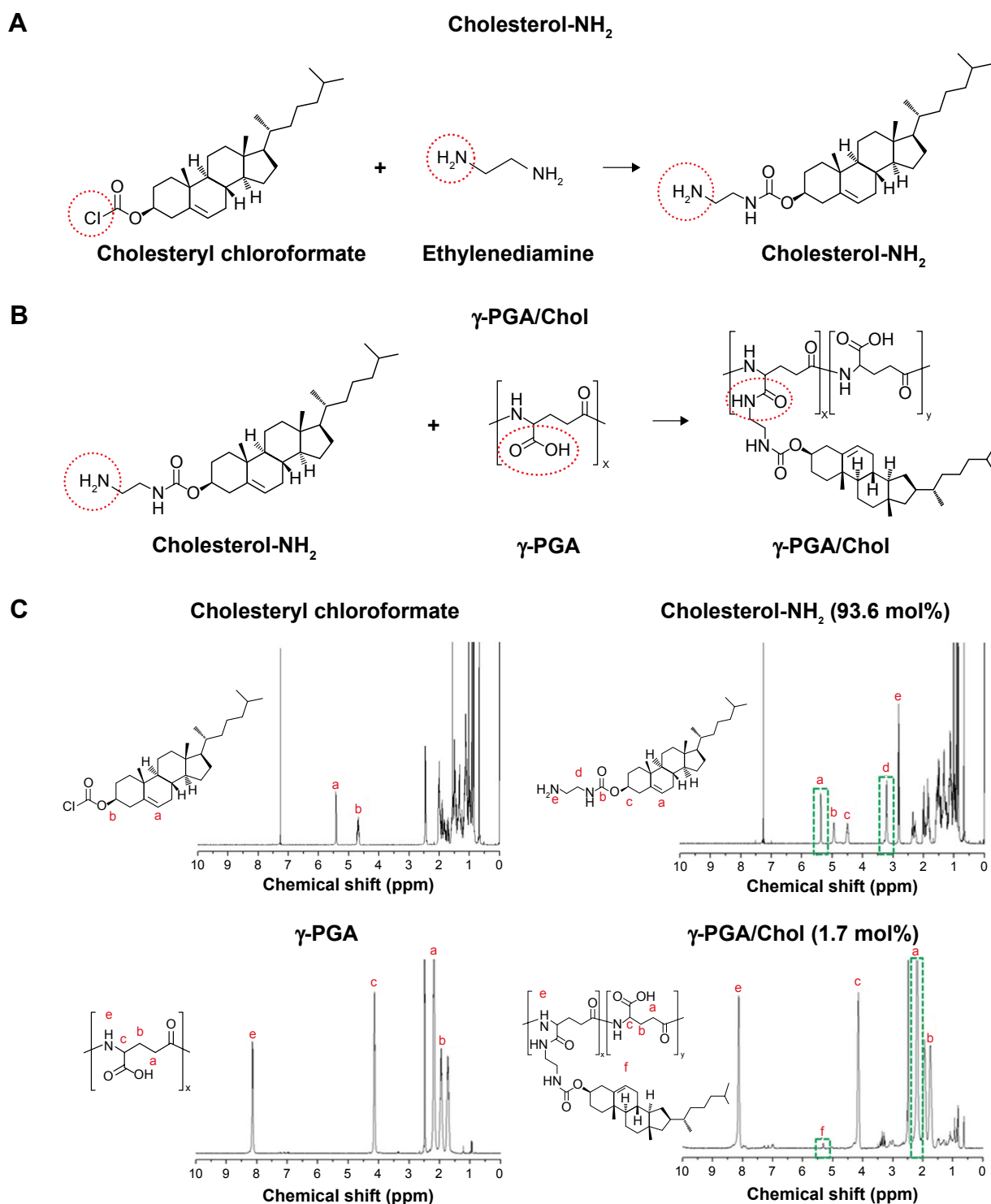


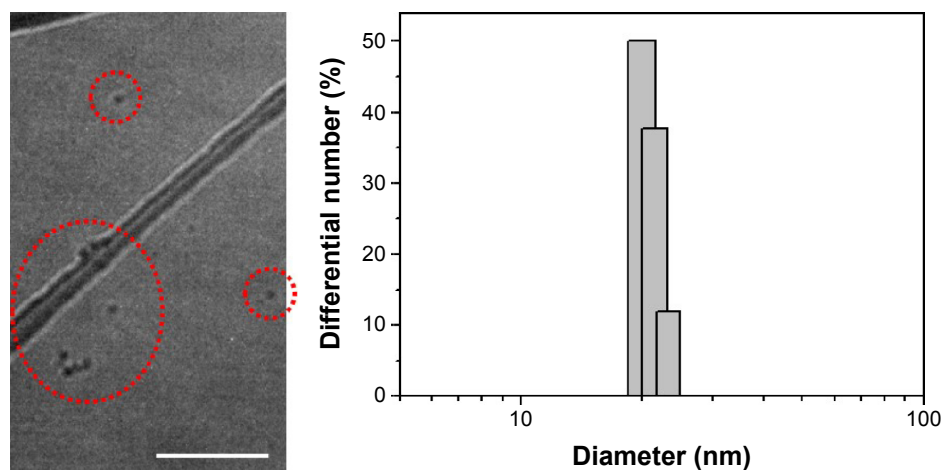
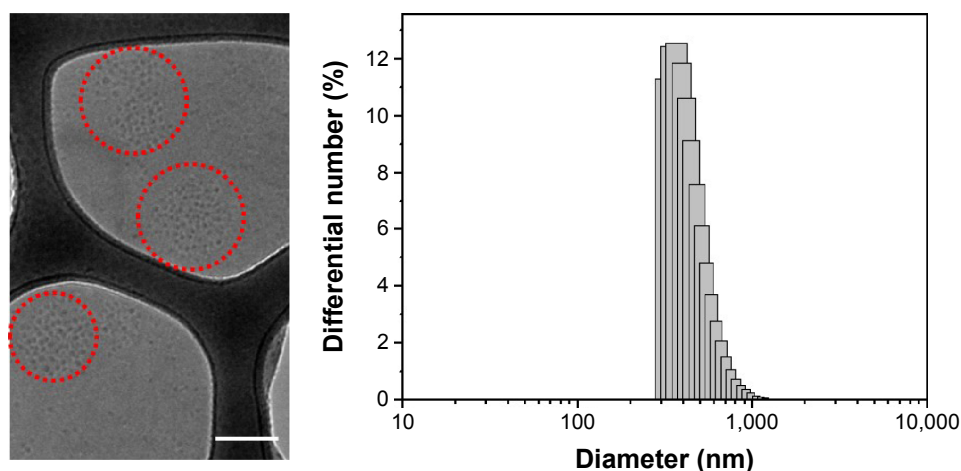
**Figure 2** Chemical scheme for the synthesis of **(A)** Cholesterol-NH<sub>2</sub> and **(B)** γ-PGA/cholesterol conjugates. **(C)** <sup>1</sup>H-NMR spectra of synthesized materials. **(C)** Letters (a–f) in <sup>1</sup>H-NMR spectra indicate peaks from hydrogens (H) in letters (a–f) located on the structure, respectively.

**Abbreviations:** γ-PGA, poly(γ-glutamic acid); <sup>1</sup>H-NMR, proton nuclear magnetic resonance; ppm, parts per million.

hydrophilic γ-PGA backbone and the hydrophobic cholesterol side chain. To conjugate the cholesterol group to the carboxyl group of γ-PGA, aminated cholesterol (cholesterol-NH<sub>2</sub>) was synthesized (Figure 2A). The methylene group of EDA (δ 3.1)

and CH=C of cholesterol-NH<sub>2</sub> (δ 5.3) were confirmed in <sup>1</sup>H-NMR spectra, indicating that the degree of substitution of cholesterol-NH<sub>2</sub> was approximately 96.2% (Figure 2C). γ-PGA conjugated with cholesterol (γ-PGA/Chol) was synthesized



**A**  $\gamma$ -PGA/Chol nanoparticles**B** RBHPs

**Figure 3** Cryo-TEM images and size distributions of **(A)**  $\gamma$ -PGA/Chol nanoparticles and **(B)** RBHPs.

**Notes:** Scale bars represent 200 nm. Circled areas show  $\gamma$ -PGA/Chol nanoparticles **(A)** and RBHPs **(B)**.

**Abbreviations:** Cryo-TEM, cryo-transmission electron microscopy;  $\gamma$ -PGA, poly( $\gamma$ -glutamic acid); Chol, cholesterol; RBHPs, raspberry-like hydrogel particles.

through the 1-ethyl-3-(3-dimethylaminopropyl)carbodiimide/N-hydroxysuccinimide coupling reaction (Figure 2B). In the  $^1\text{H}$ -NMR spectra of the  $\gamma$ -PGA/Chol conjugate, the degree of cholesterol substitution was calculated between  $\gamma\text{-CH}_2$  of  $\gamma$ -PGA ( $\delta$  2.2) and  $\text{CH}=\text{C}$  of cholesterol amine ( $\delta$  5.3) (Figure 2C). The degree of cholesterol substitution in the  $\gamma$ -PGA/Chol conjugate was approximately 1.7 mol%. When the  $\gamma$ -PGA/Chol conjugate was dispersed in aqueous solution, it formed nanoparticles and exhibited a spherical shape, with an average diameter of  $21.0 \pm 1.1$  nm (Figure 3A, Table 1). To encapsulate Dox,  $\gamma$ -PGA/Chol nanoparticles were mixed with Dox in aqueous solution. During the encapsulation process, the cationically charged Dox molecules could interact with the anionically charged carboxyl surface of the  $\gamma$ -PGA/Chol nanoparticles, ultimately forming

submicron-sized RBHPs. The size of the resultant RBHPs was  $444.9 \pm 122.5$  nm (Figure 3B, Table 1). The surface of the RBHPs showed a strong negative charge ( $-56.44$  mV) due to the presence of the carboxyl group of  $\gamma$ -PGA within

**Table 1** Physicochemical properties of  $\gamma$ -PGA/Chol nanoparticles and RBHPs (Dox-loaded  $\gamma$ -PGA/Chol nanoparticles)

Composition	Average diameter $\pm$ SD (nm) <sup>a</sup>	Zeta-potential (mV) <sup>b</sup>	Loading amount ( $\mu\text{g}/\text{mg}$ ) <sup>c</sup>
$\gamma$ -PGA/Chol nanoparticles	$21.0 \pm 1.1$	$-65.35$	—
RBHPs	$444.9 \pm 122.5$	$-56.44$	63.9

**Notes:** The values were determined by <sup>a</sup>DLS, <sup>b</sup>ELS, and <sup>c</sup>UV-vis spectrometry at  $\lambda_{\text{max}}$  498 nm. SD value was calculated in DLS equipment process from measures of 100 times.

**Abbreviations:**  $\gamma$ -PGA, poly( $\gamma$ -glutamic acid); Chol, cholesterol; DLS, dynamic light scattering; Dox, doxorubicin; ELS, electrophoretic light scattering; RBHPs, raspberry-like hydrogel particles; SD, standard deviation; UV-vis, ultraviolet-visible.

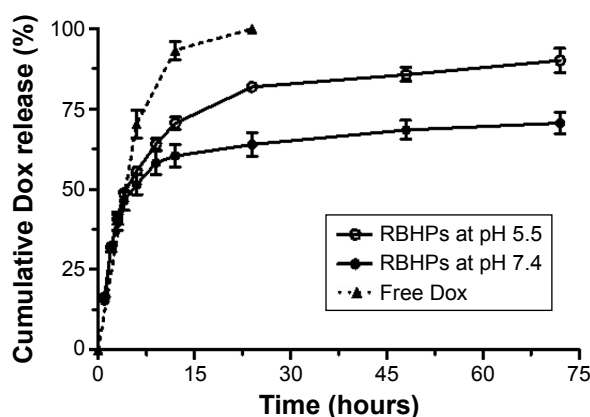


**Figure 4** In vitro release profile of free Dox in PBS and Dox from RBHPs at pH 5.5 and pH 7.4.

**Notes:** The release of Dox was determined by a dialysis method. Error bars were expressed using standard deviation from measures of 3 repetition ( $n=3$ ).

**Abbreviations:** Dox, doxorubicin; PBS, phosphate-buffered saline; RBHPs, raspberry-like hydrogel particles.

the shell of the nanoparticles. The loaded amount of Dox was  $\sim 63.9 \mu\text{g}/\text{mg}$  of RBHPs (Table 1).

## In vitro release of Dox from RBHPs

Figure 4 shows the in vitro release profiles of Dox released from RBHPs, as determined by a dialysis method in PBS (pH 7.4). The amount of Dox released was  $20.38\% \pm 2.05\%$  at 6 h, and the RBHPs continuously released  $61.5\% \pm 1.5\%$  of the loaded Dox over a period of 3 days. The RBHPs exhibited slow and sustained release patterns because of the diffusion of Dox from the hydrogel structure of the RBHPs. Because the  $\gamma$ -PGA/Chol nanoparticles contain a combination of carboxyl groups and hydrophobic cholesterol groups, the deprotonated carboxylate groups are partially protonated at the endosomal and lysosomal pH range. By the protonation of carboxylate groups, the electrostatic interaction between the  $\gamma$ -PGA/Chol and Dox became weak at the acidic pH and Dox could be released from the RBHPs. We could demonstrate this phenomenon from the result that Dox was released more quickly from the hydrogel particles at pH 5.5 than at pH 7.4.

## Cellular uptake and endosome-disruptive properties of RBHPs

To investigate the cellular uptake and cytotoxic effect, various concentrations of RBHPs (containing  $0.05$ – $20 \mu\text{g}/\text{mL}$  Dox) were added to HeLa cells (a human cervical cancer cell line) for 4 or 24 h. The in vitro cellular uptake efficiency of the RBHPs was evaluated by fluorescence microscopy and flow cytometry (Figure 5). After 4 h, strong fluorescence of free Dox was observed in the cell nuclei, whereas a weak signal was observed in the cytoplasm, suggesting that most free Dox

rapidly diffused into the cell nuclei (Figure 5A). In contrast, the fluorescence signal from Dox was observed in both the cytosol and nuclei at both 4 and 24 h when the HeLa cells were treated with RBHPs (Figure 5). These results indicated that Dox is being released from RBHPs intracellularly and is being diffused to the nucleus, where it acts in analogy to free Dox. Based on the flow cytometry results, the cellular uptake of Dox was slightly higher in the case of the RBHP-treated HeLa cells than in the case of free Dox (Figure 5B). But, the result was not statistically significant. To investigate the intracellular delivery of Dox into cytosolic compartments, we characterized the localization of RBHPs after entering HeLa cells. As shown in Figure 6A, red signals from Dox were observed throughout the cells, and the line profile and image analysis indicated that Dox (red,  $\lambda_{\text{em}} = 605 \text{ nm}$ ) was located in the nucleus (part 1) and in the cytosolic compartments (part 2), whereas Dox was also colocalized to the lysosome (part 3, overlay of Dox [red,  $\lambda_{\text{em}} = 605 \text{ nm}$ ] and LysoTracker<sup>®</sup> [blue,  $\lambda_{\text{em}} = 455 \text{ nm}$ ]). The experimental results suggest that Dox can be released from RBHPs in a controlled manner and can affect cells for a longer time than free Dox. To investigate the capacity of RBHPs for membrane disruption and Dox delivery into cytosolic compartments, we adopted a standard hemolysis assay. The pH-dependent membrane-destabilizing properties of the RBHPs and  $\gamma$ -PGA/Chol nanoparticles were evaluated using this standard hemolysis assay (Figures 6B and S1). As shown in Figure 6B, hemolysis started at pH 6.5 and increased drastically at pH 6.0–5.5 ( $\sim 65\%$ ), whereas there was no hemolysis at pH 7.4. The RBHPs contained  $\gamma$ -PGA/Chol nanoparticles composed of hydrophilic deprotonated carboxyl groups and hydrophobic cholesterol groups. These nanoparticles formed a stable micelle-like structure due to the hydrophilic–hydrophobic balance at physiological pH (pH 7.4). However, the hydrophobic character increased due to both the increased number of protonated carboxyl groups in the shell and the intrinsically hydrophobic cholesterol core at endosomal and/or lysosomal pH (Figure 7). However, no hemolysis effect was observed when free  $\gamma$ -PGA polymers (with 50 kDa and 500 kDa) were used (Figure 6B). Upon this increase in hydrophobicity, the RBHPs containing the polymer nanoparticles easily interact with and penetrate cell membranes and destabilize them.

## Cytotoxicity of RBHPs

The cytotoxic effect of both free Dox and RBHPs was dependent on the concentration and duration of Dox treatment. The cytotoxic effect of RBHPs was similar to that of free Dox up to 4 h at all concentrations of Dox (Figure 8A).

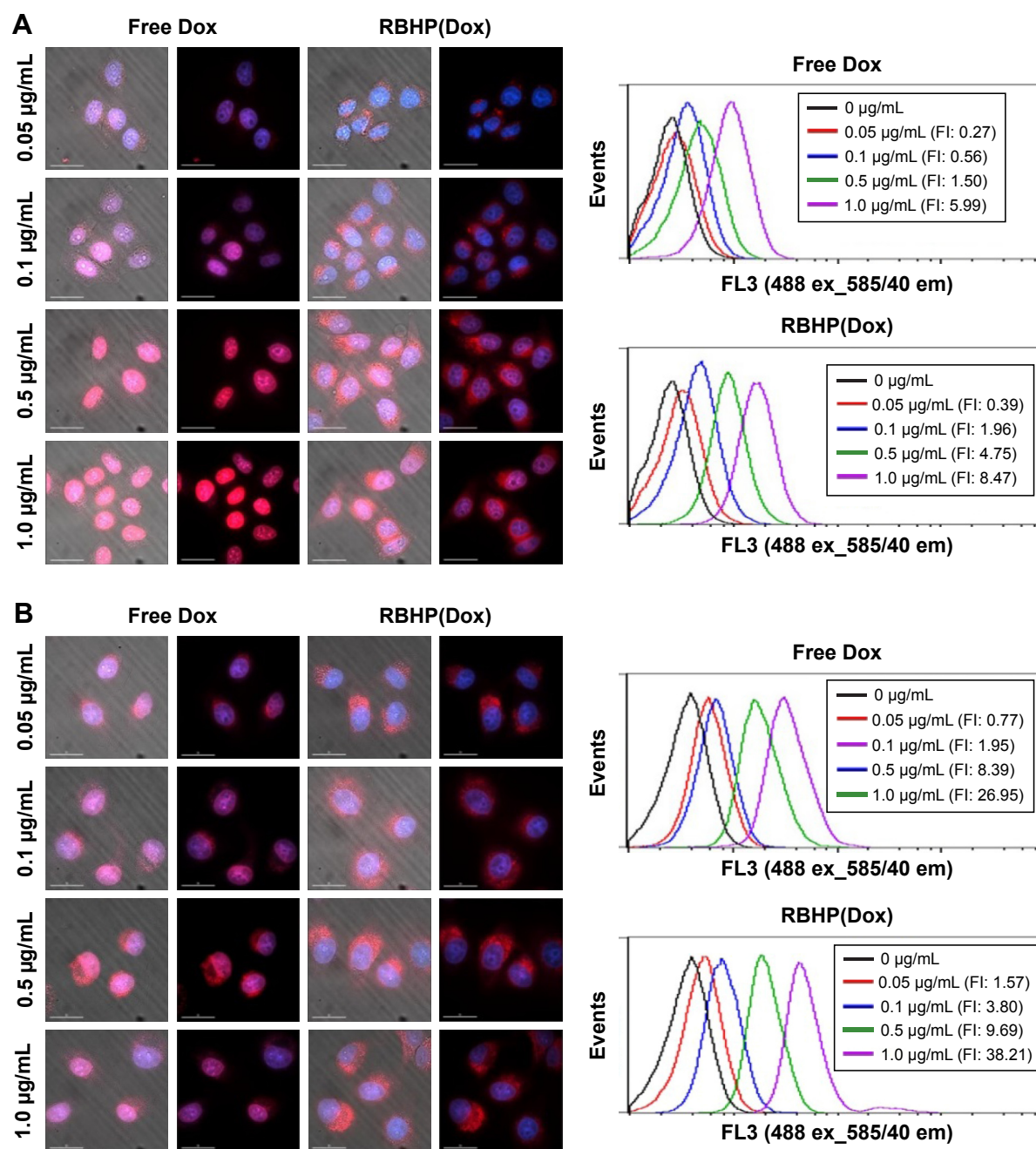


**Figure 5** In vitro cellular uptake studies of Dox in HeLa cells.

**Notes:** Dox solution and RBHPs were incubated for **(A)** 4 h and **(B)** 24 h. Cellular uptake and distribution of Dox were examined by fluorescence microscopy. Cell nuclei were stained by DAPI (blue) and red color indicates Dox. Exposure time for each experiment was varied to maximize the difference between free Dox and RBHP(Dox) (scale bars =30 µm). **(A)** Exposure time was 0.15 s for DAPI signal and 1 s for Dox signal. **(B)** Exposure time was 0.15 s for DAPI signal and 0.25 s for Dox signal.

**Abbreviations:** h, hours; Dox, doxorubicin; RBHPs, raspberry-like hydrogel particles; DAPI, 4',6-diamidino-2-phenylindole; RBHP(Dox), Dox encapsulated in RBHP; FI, fluorescence intensity.

However, the cytotoxic effects of RBHPs were shown in a slower manner after 24 h of treatment, due to the sustained release of Dox from the RBHPs (Figure 8B). Taken together, the results suggest that RBHPs can be used as nanocarriers for cytosolic delivery of anticancer drugs due to their high intracellular delivery capacity and their controlled release of encapsulated Dox. Furthermore, if we consider the fact that a drug delivery carrier intended for clinical applications should

use materials that are safe as pharmaceutical excipients,  $\gamma$ -PGA-based hydrogel particles would be referred to as a good candidate due to their excellent biocompatibility.

## Conclusion

We have developed RBHPs for the cytosolic delivery of anticancer drugs making use of the pH-dependent membrane-disrupting property of RBHPs. The RBHPs were



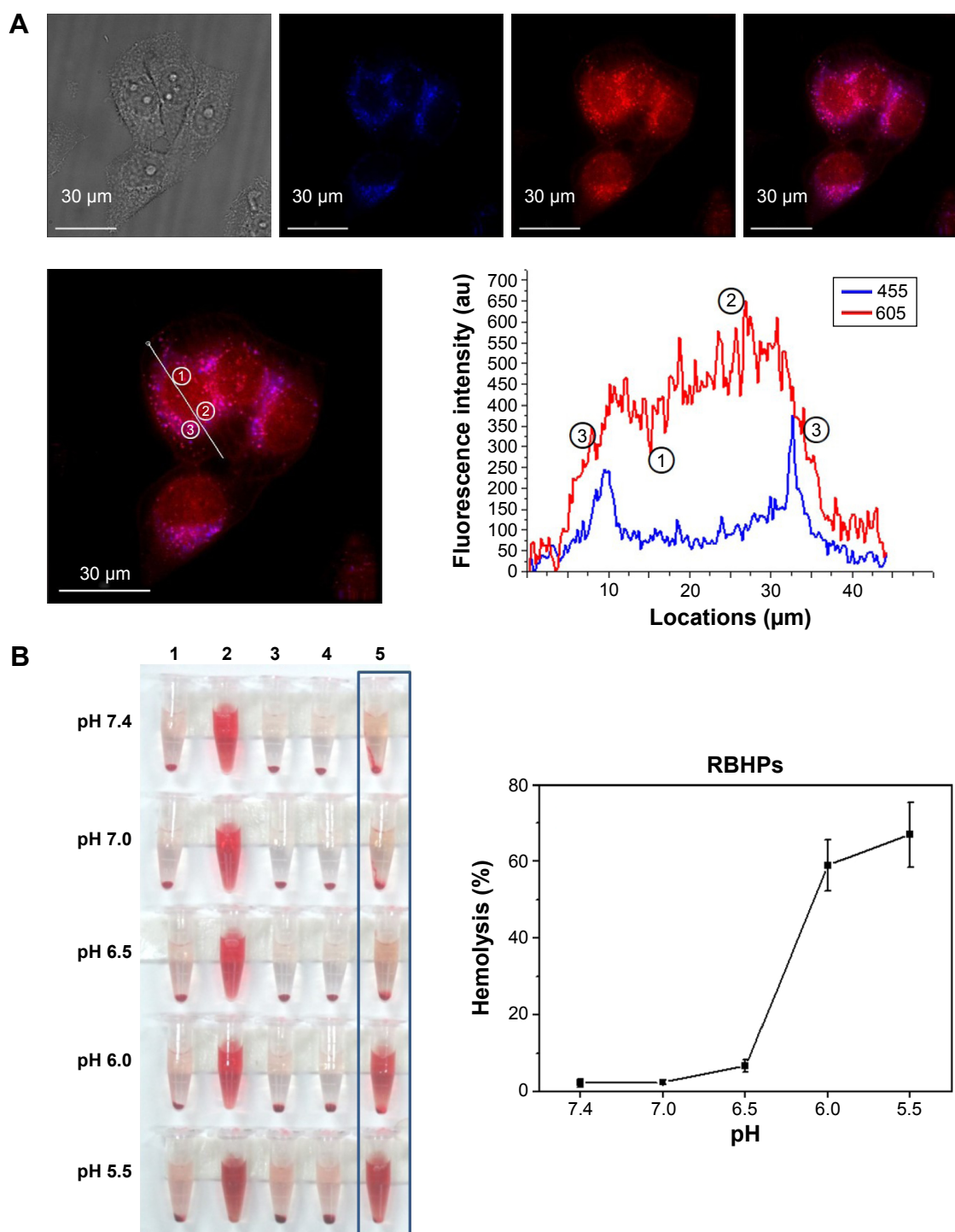


**Figure 6** pH-dependent membrane disruption and cytosolic delivery capacity of RBHPs.

**Notes:** (A) Localization of Dox at 4 h after intracellular delivery of RBHPs: some Dox (red,  $\lambda_{em} = 605$  nm) is located in the nucleus (part 1) and cytosolic compartments (part 2), whereas other Dox moieties are co-localized in the lysosome (part 3, overlay of doxorubicin [red,  $\lambda_{em} = 605$  nm] and LysoTracker® [blue,  $\lambda_{em} = 455$  nm]). (B) Hemolysis results (column 1: PBS; column 2: 0.2% Triton X; column 3: 50 kDa  $\gamma$ -PGA; column 4: 500 kDa  $\gamma$ -PGA; column 5: RBHPs). Left panel is representative image of hemolysis results. Right panel is relative value for hemolysis after treatment of RBHPs (absorbance of hemoglobin in the supernatant from 0.2% Triton X experimental group was 100% and error bars were expressed as mean  $\pm$  standard deviation values from  $n=3$ ).

**Abbreviations:** h, hours; Dox, doxorubicin; RBHPs, raspberry-like hydrogel particles; PBS, phosphate-buffered saline;  $\gamma$ -PGA, poly( $\gamma$ -glutamic acid).

formed by the electrostatic interaction between building blocks (ie,  $\gamma$ -PGA nanoparticles with a carboxylate surface) and cross-linkers (cationically charged anticancer drugs). The RBHPs showed controlled drug release behavior in

both in vitro and ex vivo cell experiments, with a cytotoxic effect that was dependent on both the concentration and the duration of RBHP treatment. The cytosolic delivery capacity of the RBHPs was analyzed based on their pH-dependent

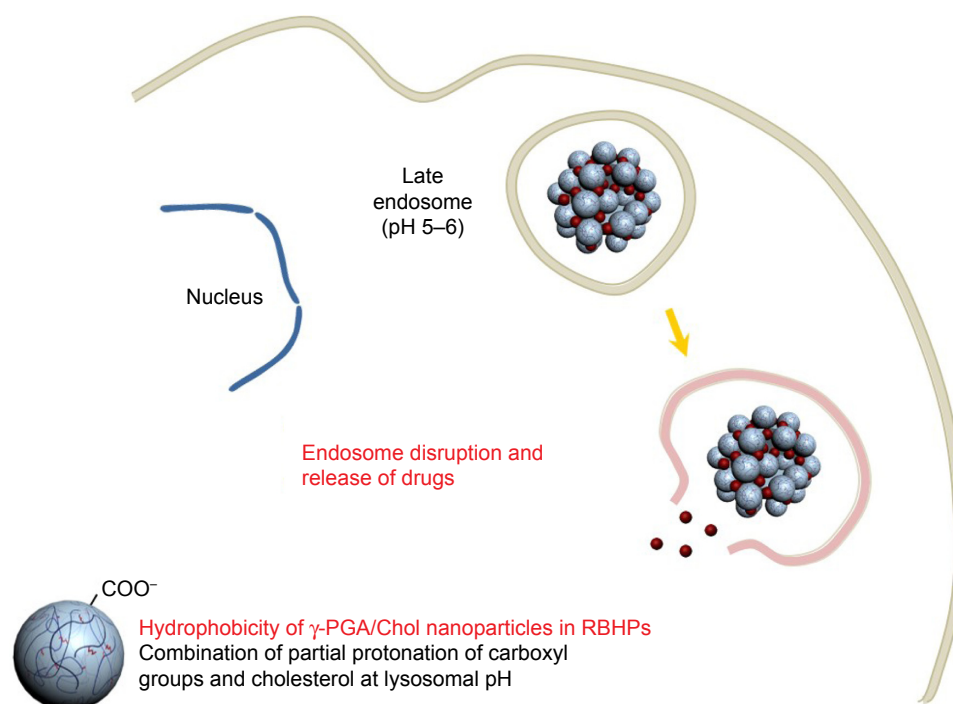


**Figure 7** Scheme for the cytosolic delivery of RBHPs formed by the self-assembling polymeric nanoparticles and antitumor drugs.

**Note:** Due to the increased hydrophobicity of RBHPs at lysosomal acidic pH, RBHPs can easily interact, penetrate, and destabilize cell membranes, as well as release encapsulated drugs.

**Abbreviations:** RBHPs, raspberry-like hydrogel particles;  $\gamma$ -PGA, poly( $\gamma$ -glutamic acid); Chol, cholesterol.

membrane-disrupting character, which was evaluated using a standard hemolysis assay. In fact, we loaded drugs into hydrogel particles using the electrostatic interaction between positively charged Dox with negatively charged  $\gamma$ -PGA/Chol hydrogel nanoparticles. To expand the applicability of  $\gamma$ -PGA/Chol hydrogel nanoparticles as drug delivery

carriers for various drugs that have different physical and chemical properties, the carboxylate group of  $\gamma$ -PGA can be modified with various chemical groups such as amine, thiol, and aldehyde moieties. In case of hydrophobic drugs, they can be encapsulated into the hydrophobic cholesterol part of the  $\gamma$ -PGA/Chol hydrogel nanoparticles. Based on

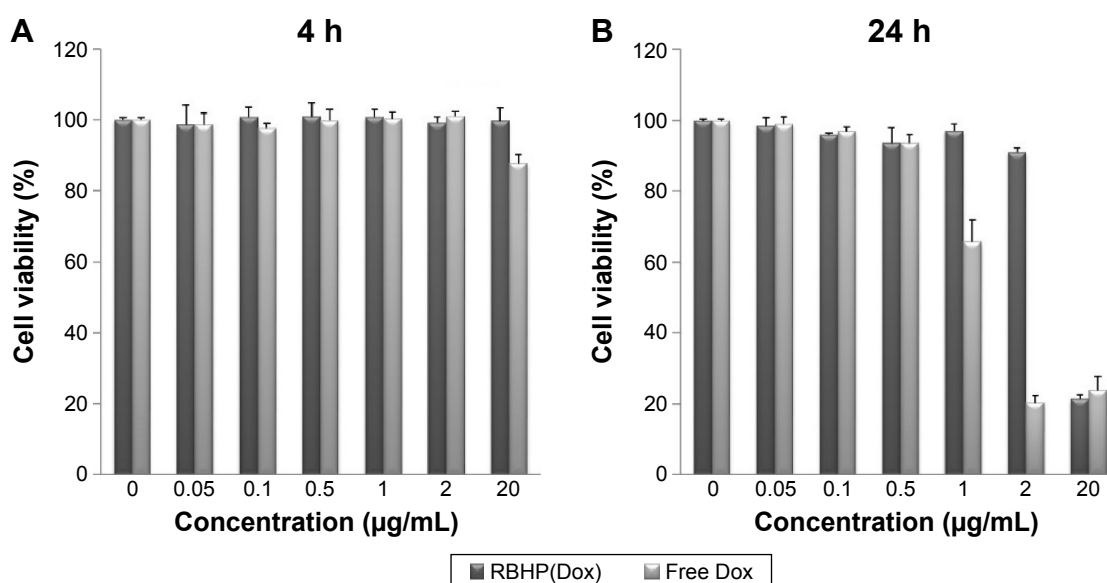


**Figure 8** Cytotoxicity of free Dox and RBHP(Dox) at (A) 4 h and (B) 24 h.

**Note:** HeLa cell viability was measured by the MTS assay.

**Abbreviations:** h, hours; Dox, doxorubicin; RBHPs, raspberry-like hydrogel particles; MTS, methyl tetrazolium salt; RBHP(Dox), Dox encapsulated in RBHP.

the experimental results, RBHPs are expected to be used as controlled cytosolic delivery carriers after loading with other therapeutic drugs or active compounds.

## Acknowledgments

This work was supported by financial support from the National Research Foundation of Korea (NRF) funded by the Korean government (MEST) (numbers 2014R1A2A1A10049960 and 2015R1A2A1A15051980); a grant from the Korea Health Technology R&D Project, provided through the Korea Health Industry Development Institute, funded by the Ministry of Health and Welfare (grant number HI14C2680); and the National Research Council of Science and Technology grant by the Korea government (MSIP) (number CAP-15-09-KIMS).

## Disclosure

The authors report no conflicts of interest in this work.

## References

- Brigger I, Dubernet C, Couvreur P. Nanoparticles in cancer therapy and diagnosis. *Adv Drug Deliv Rev.* 2002;54(5):631–651.
- Ferrari M. Cancer nanotechnology: opportunities and challenges. *Nat Rev Cancer.* 2005;5(3):161–171.
- Park JH, Lee S, Kim J-H, Park K, Kim K, Kwon IC. Polymeric nanomedicine for cancer therapy. *Prog Polym Sci.* 2008;33(1):113–137.
- Park K, Lee GY, Kim YS, et al. Heparin-deoxycholic acid chemical conjugate as an anticancer drug carrier and its antitumor activity. *J Control Release.* 2006;114(3):300–306.
- Tyrrell ZL, Shen YQ, Radosz M. Fabrication of micellar nanoparticles for drug delivery through the self-assembly of block copolymers. *Prog Polym Sci.* 2010;35(9):1128–1143.
- Eckmann DM, Composto RJ, Tsourkas A, Muzykantov VR. Nanogel carrier design for targeted drug delivery. *J Mater Chem B Mater Biol Med.* 2014;2(46):8085–8097.
- Hamidi M, Azadi A, Rafiei P. Hydrogel nanoparticles in drug delivery. *Adv Drug Deliv Rev.* 2008;60(15):1638–1649.
- Zhang H, Tian Y, Zhu Z, et al. Efficient antitumor effect of co-drug-loaded nanoparticles with gelatin hydrogel by local implantation. *Sci Rep.* 2016;6:26546.
- Kabanov AV, Vinogradov SV. Nanogels as pharmaceutical carriers: finite networks of infinite capabilities. *Angew Chem Int Ed Engl.* 2009;48(30):5418–5429.
- Raemdonck K, Demeester J, De Smedt S. Advanced nanogel engineering for drug delivery. *Soft Matter.* 2009;5(4):707–715.
- Buescher JM, Margaritis A. Microbial biosynthesis of polyglutamic acid biopolymer and applications in the biopharmaceutical, biomedical and food industries. *Crit Rev Biotechnol.* 2007;27(1):1–19.
- Lee EH, Kamigaito Y, Tsujimoto T, Uyama H, Sung MH. Synthesis of an amphiphilic poly(gamma-glutamic acid)-cholesterol conjugate and its application as an artificial chaperone. *J Microbiol Biotechnol.* 2010;20(10):1424–1429.
- Bae SR, Park C, Choi JC, Poo H, Kim CJ, Sung MH. Effects of ultra high molecular weight poly-gamma-glutamic acid from bacillus subtilis (chungkookjang) on corneal wound healing. *J Microbiol Biotechnol.* 2010;20(4):803–808.
- Baek S, Singh RK, Khanal D, et al. Smart multifunctional drug delivery towards anticancer therapy harmonized in mesoporous nanoparticles. *Nanoscale.* 2015;7(34):14191–14216.
- Biswas S, Kumari P, Lakhani PM, Ghosh B. Recent advances in polymeric micelles for anti-cancer drug delivery. *Eur J Pharm Sci.* 2016;83:184–202.
- Chen Z. Small-molecule delivery by nanoparticles for anticancer therapy. *Trends Mol Med.* 2010;16(12):594–602.
- Fang RH, Hu CMJ, Luk BT, et al. Cancer cell membrane-coated nanoparticles for anticancer vaccination and drug delivery. *Nano Lett.* 2014;14(4):2181–2188.
- Oerlemans C, Bult W, Bos M, Storm G, Nijssen JFW, Hennink WE. Polymeric micelles in anticancer therapy: targeting, imaging and triggered release. *Pharm Res.* 2010;27(12):2569–2589.
- Wilczewska AZ, Niemirowicz K, Markiewicz KH, Car H. Nanoparticles as drug delivery systems. *Pharmacol Rep.* 2012;64(5):1020–1037.
- Nochi T, Yuki Y, Takahashi H, et al. Nanogel antigenic protein-delivery system for adjuvant-free intranasal vaccines. *Nat Mater.* 2010;9(7):572–578.
- Okamoto S, Matsuura M, Akagi T, et al. Poly(gamma-glutamic acid) nano-particles combined with mucosal influenza virus hemagglutinin vaccine protects against influenza virus infection in mice. *Vaccine.* 2009;27(42):5896–5905.
- Ishi-i T, Iguchi R, Snip E, Ikeda M, Shinkai S. [60]fullerene can reinforce the organogel structure of porphyrin-appended cholesterol derivatives: novel odd-even effect of the (CH<sub>2</sub>)<sub>n</sub> spacer on the organogel stability. *Langmuir.* 2001;17(19):5825–5833.
- Lee EH, Son WC, Lee SE, Kim BH. Anti-obesity effects of poly-gamma-glutamic acid with or without isoflavones on high-fat diet induced obese mice. *Biosci Biotechnol Biochem.* 2013;77(8):1694–1702.
- Li L, Gao FP, Tang HB, et al. Self-assembled nanoparticles of cholesterol-conjugated carboxymethyl curdlan as a novel carrier of epirubicin. *Nanotechnology.* 2010;21(26):265601.
- Seo J-H, Kim C-S, Lee S-P. Physicochemical properties of poly-γ-glutamic acid produced by a novel *Bacillus subtilis* HA isolated from Cheonggukjang. *Prev Nutr Food Sci.* 2008;13(4):354–361.
- Shin EJ, Sung MJ, Park JH, et al. Poly-gamma-glutamic acid induces apoptosis via reduction of COX-2 expression in TPA-induced HT-29 human colorectal cancer cells. *Int J Mol Sci.* 2015;16(4):7577–7586.

## Supplementary material

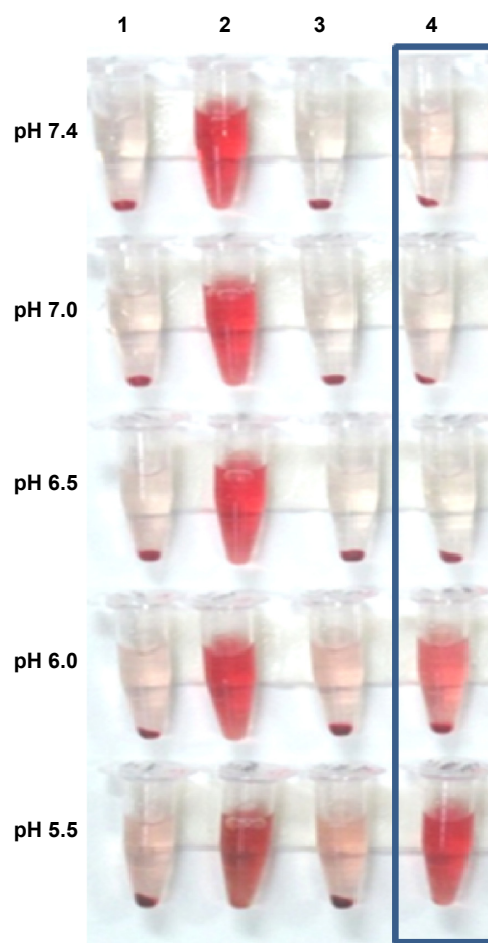


**Figure S1** Results of hemolysis with  $\gamma$ -PGA/Chol nanoparticles.

**Notes:** 1, PBS; 2, 0.2% Triton X; 3,  $\gamma$ -PGA; 4,  $\gamma$ -PGA/Chol nanoparticles.

**Abbreviations:**  $\gamma$ -PGA, poly( $\gamma$ -glutamic acid); Chol, cholesterol; PBS, phosphate-buffered saline.

### International Journal of Nanomedicine

Dovepress

### Publish your work in this journal

The International Journal of Nanomedicine is an international, peer-reviewed journal focusing on the application of nanotechnology in diagnostics, therapeutics, and drug delivery systems throughout the biomedical field. This journal is indexed on PubMed Central, MedLine, CAS, SciSearch®, Current Contents®/Clinical Medicine,

Journal Citation Reports/Science Edition, EMBase, Scopus and the Elsevier Bibliographic databases. The manuscript management system is completely online and includes a very quick and fair peer-review system, which is all easy to use. Visit <http://www.dovepress.com/testimonials.php> to read real quotes from published authors.

Submit your manuscript here: <http://www.dovepress.com/international-journal-of-nanomedicine-journal>